J. Phys. Chem. A **2003,** *107,* 4445−4451

Nanosecond Laser Photolysis of Ni(II) Tetraphenylporphyrin. Kinetic Studies on Association and Dissociation of Aliphatic Amines at the Axial Positions

Hiroyuki Suzuki,[†,‡] Haruna Adachi,[†,‡] Yoshio Miyazaki,[§] and Mikio Hoshino*,[†,‡]

The Institute of Physical and Chemical Research, Wako, Saitama 351- 0198, Japan, and Interdisciplinary Graduate School of Science and Engineering, Tokyo Institute of Technology, Nagatsuda-machi, Midori-ku, Yokohama, Kanagawa 226-8502, Japan, and Department of Chemistry, Faculty of Engineering, Toyo University, Kujirai, Kawagoe, Saitama 350-8585, Japan

Received: August 19, 2002; In Final Form: February 12, 2003

Nanosecond laser photolysis studies of nickel(II) tetraphenylporphyrin, $Ni^{II}TPP$, in toluene solutions containing primary, secondary, and tertiary aliphatic amines were carried out for elucidation of the association and dissociation mechanisms of the axial amines. From the absorption spectroscopic studies, the primary amines were found to react with $Ni^{II}TPP$ to give the six coordinate species. The secondary and the tertiary amines, however, give no coordinated species. The laser photolysis of $Ni^{II}TPP$ in toluene containing primary amines revealed that the four- and six-coordinate species undergo mutual exchange upon laser excitation. In secondary amine−toluene solutions, the four coordinated species undergoes light-induced transformation to yield the six-coordinate species. However, no formation of the six coordinate species are observed for tertiary amine−toluene solutions of $Ni^{II}TPP$ by photolysis. The six and four coordinate species produced by laser photolysis of the amine−toluene solutions decay according to the pseudo-first-order kinetics. The plot of the rate constant, k_{obsd}, for the decay of these transient species vs the primary amine concentration at 300 K is concave upward: the value k_{obsd} initially decreases toward a minimum and then increases with an increase in the amine concentration. Because the laser photolysis of $Ni^{II}TPP$ in primary amine−toluene solutions results in the nonequilibrium state among four and six-coordinate species, k_{obsd} is the rate constant to reach the equilibrium state. It is assumed that the four and six coordinate species in the nonequilibrium state achieve the equilibrium via the formation of a five coordinate $Ni^{II}TPP$ as an intermediate. The rate constants, k_{obsd}, represented as a function of the primary amine concentration are well explained with the use of the steady-state approximation with regard to the five coordinate species. On the basis of the laser photolysis in the temperature range 200−300 K, the reaction mechanisms for the equilibrium reactions between $Ni^{II}TPP$ and various amines are discussed in detail.

Introduction

Photoinduced dissociation of axial ligands from various metalloporphyrins has been the subject of extensive studies[1−19] partly because of their importance for elucidation of the thermal association and dissociation mechanisms of the axial ligands in heme proteins.[20−30] In contrast to the photodissociation, only a few reports have been made for the photoinduced association of the axial ligand to metalloporphyrins.[3,31−33] Among various metalloporphyrins, Ni(II)tetraphenylporphyrin ($Ni^{II}TPP$) is the typical molecule which exhibits both association and dissociation of axial ligands upon laser excitation.[3,33]

The central Ni(II) atom in nickel(II) porphyrins has the d^8 electron configuration. Four coordinate $Ni^{II}TPP$ is known to have the $^1A_{1g}$ $((d_{z^2})^2)$ in the ground state.[34,35] The orange red toluene solution of $Ni^{II}TPP$ exhibits no appreciable change in color in the presence of 2.0 M pyridine at room temperature. However, when the solution is cooled to 200 K, the color of the solution turns from orange red to violet because of the formation of $(Py)_2Ni^{II}TPP$ (Py = pyridine at the axial position), which has the $^3B_{1g}$ $(d_{z^2}{}^1, d_{x^2-y^2}{}^1)$ state. The absorption spectroscopic and NMR studies have demonstrated that the four-, five-, and six- coordinate Ni porphyrins are in equilibrium in the organic solvents containing nitrogen bases.[36]

The excited states of nickel(II) porphyrins, $Ni^{II}P$, responsible for association and dissociation of the ligand molecule have been examined by pico- and femtosecond photolysis.[3,7,37−40] The lowest excited state of $Ni^{II}P$ has been identified as the metal excited state, from which dissociation and association of the axial ligand takes place. In the present study, we have carried out laser photolysis studies of $Ni^{II}TPP$ in aliphatic amine−toluene solutions. The dissociation and the association mechanisms of aliphatic amines to $Ni^{II}TPP$ are investigated on the basis of the kinetic studies of the transient species.

Experimental Section

Reagent grade toluene was used as a solvent without further purification. Purified $Ni^{II}TPP$ was kindly donated by Dr. Yamamoto of our institute. Aliphatic amines and pyridine derivatives (2-, 3-, and 4-methylpyridine) were purified by distillation under reduced pressure before use. The concentrations of $Ni^{II}TPP$ used in the present study are $2.0-3.0 \times 10^{-6}$ M.

Absorption spectra were recorded on a Hitachi 330 spectrophotometer. The temperature of the sample solution was controlled by a cryostat from Oxford Instruments (DN 1001).

The laser photolysis was performed with the use of third harmonics from the YAG laser (HY500 from JK Lasers Ltd.). The duration and the energy of the laser pulse are 20 ns and

---

* To whom correspondence should be addressed. Fax: 048-462-4668. Phone: 048-467-9426. E-mail: hoshino@postman.riken.go.jp.
[†] The Institute of Physical and Chemical Research.
[‡] Tokyo Institute of Technology.
[§] Toyo University.

10.1021/jp0219000 CCC: $25.00

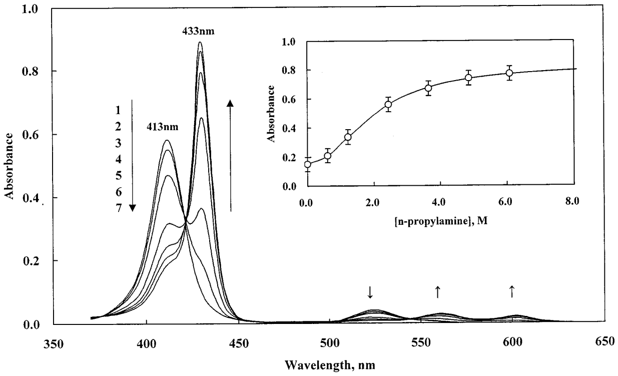

Figure 1. Absorption spectral changes observed for $Ni^{II}TPP$ in toluene by changing [*n*-propylamine]: (1) 0.0, (2) 0.61, (3) 1.2, (4) 2.4, (5) 3.65, (6) 4.9, and (7) 6.1 M. The inset shows the absorbance at 413 nm represented as a function of [*n*-propylamine]. The solid line is the calculated curve with the use of $K = 0.25\ M^{-2}$.

100 mJ/pulse, respectively. The transient spectra were taken by the intensified charge coupled device detector.[18,19] The decay of the transient spectrum was measured with a photomultiplier (Hamamatsu R 758). The monitoring light from a xenon lamp (Ushio 150 D, 150 W) was led to the entrance slit of the monochromator. Then, the monochromated light intensity from the exit of the monochromator was detected by the photomultiplier. The output from the photomultiplier was conducted to the digital storage oscilloscope (Gould model 630 from Gould Instrument System, Ltd.). The data were stored on a personal computer for kinetic analysis.

Results

Absorption Spectral Changes of $Ni^{II}TPP$ in Amine−Toluene Solutions. The absorption spectrum of $Ni^{II}TPP$ in toluene solutions exhibits marked changes by addition of primary aliphatic amines. The spectral changes are found to be very similar independent of the nature of the primary amine used.

Figure 1 shows the absorption spectral changes observed for $Ni^{II}TPP$ in toluene containing 0−6.1 M *n*-propylamine, *n*-PA. The absorption peaks of $Ni^{II}TPP$ located at 413 and 525 nm shift toward red with an increase in the concentration of *n*-propylamine, [*n*-PA], and new peaks appear at 433, 563, and 603 nm with isosbestic points. According to earlier spectroscopic studies,[41−46] the new peaks are ascribed to the six coordinate species, $(n\text{-PA})_2\ Ni^{II}TPP$. The spectral changes observed for the *n*-propylamine−toluene solutions are interpreted in terms of the equilibrium reactions described below

$$Ni^{II}TPP + n\text{-PA} \overset{K_1}{\rightleftharpoons} (n\text{-PA})Ni^{II}TPP \quad (1)$$

$$(n\text{-PA})Ni^{II}TPP + n\text{-PA} \overset{K_2}{\rightleftharpoons} (n\text{-PA})_2Ni^{II}TPP \quad (2)$$

Because isosbestic points appear in the spectral changes, we concluded that the equilibrium reaction is composed of two major species, $Ni^{II}TPP$ and $(n\text{-PA})_2\ Ni^{II}TPP$. Presumably, the concentration of the five coordinate species, $(n\text{-PA})Ni^{II}TPP$ is too low to be detected by absorption spectroscopy: $[(n\text{-PA})Ni^{II}TPP] \ll [Ni^{II}TPP] + [(n\text{-PA})_2Ni^{II}TPP]$. The absorbance change at 433 nm is represented as a function of [*n*-PA] in the inset of Figure 1. From eqs 1 and 2 and $[(n\text{-PA})Ni^{II}TPP] \ll [Ni^{II}TPP] + [(n\text{-PA})_2Ni^{II}TPP]$, the 433-nm absorbance, D, is formulated as

$$D = (D_0 + D_\infty K[n\text{-PA}]^2)/(1 + K[n\text{-PA}]^2) \quad (3)$$

Here D_0 and D_∞ denote the 433-nm absorbance at $[n\text{-PA}] = 0$ and at an "infinite" concentration of *n*-PA, respectively. From K_1 and K_2, K is given by $K = K_1K_2$. With the use of the curve fitting and least-squares method, K is obtained as $0.25\ M^{-2}$. The sum of square residuals, $\sum e_i^2$, was 7.29×10^{-5}.

The similar absorption spectral changes of $Ni^{II}TPP$ in toluene solutions were measured by changing the concentration of aromatic amines, 3- and 4-methylpyridine. The spectral changes are very close to those observed with primary amines. However, the addition of 2-methylpyridine gives no effects on the absorption spectrum of $Ni^{II}TPP$ in toluene, indicating that methyl group at the 2 position prohibited the coordination of 2-methylpyridine to the axial positions of $Ni^{II}TPP$. The addition of the secondary and tertiary amines does not affect the absorption spectrum of $Ni^{II}TPP$ in toluene: neither the shift of the absorption peaks nor the change in the molar absorption coefficients was detected for $Ni^{II}TPP$ even at 8.0 M amines. Thus, the species in these solutions is concluded to be $Ni^{II}TPP$.

Laser Photolysis of $Ni^{II}TPP$ in Amine−Toluene Solutions at Room Temperature. Laser photolysis studies were carried out for $Ni^{II}TPP$ in primary amine−toluene solutions by changing the concentration of the amines. With an increase in the amine concentration, the ratio, $[Ni^{II}TPP]$/[six coordinate $Ni^{II}TPP$], decreases. When the amine concentration is low, the transient spectrum observed at 30 ns after the pulse has a positive peak at ca. 430 nm and a negative one at ca. 415 nm. On the other hand, at high amine concentrations, the transient spectra measured at 30 ns exhibit a positive peak at ca. 415 and a negative one at ca. 430 nm in the Soret band region. Taking account of the absorption spectral changes of $Ni^{II}TPP$ in the presence of primary amines, we concluded that, upon laser excitation, four-coordinate species and six-coordinate species interconvert each other. The transient spectra uniformly decay according to first-order kinetics over the wavelength region studied. As an example, the laser photolysis of $Ni^{II}TPP$ in cyclohexylamine−toluene solutions is described below. The absorption spectrum of $Ni^{II}TPP$ changes with an increase in the concentration of cyclohexylamine, CHA. From the absorption spectral measurements, the major species at 0.88 and 4.4 M CHA are $Ni^{II}TPP$ and $(CHA)_2Ni^{II}TPP$, respectively. Figure 2 shows the transient absorption spectra of $Ni^{II}TPP$ in cyclohexylamine−toluene solutions taken at 30 ns after the 355-nm laser pulse. The spectrum (A) observed for the toluene solution of $Ni^{II}TPP$ containing 0.88 M CHA is in good agreement with the difference spectrum, $(CHA)_2Ni^{II}TPP$ minus $Ni^{II}TPP$. When the toluene solution of $Ni^{II}TPP$ contains 4.4 M CHA, the transient spectrum (B) is in accord with the difference spectrum, $Ni^{II}TPP$ minus $(CHA)_2Ni^{II}TPP$. Thus, in appearance, the photochemical reaction of this system is represented as

$$Ni^{II}TPP + 2CHA + h\nu \rightarrow (CHA)_2Ni^{II}TPP \quad (4)$$

$$(CHA)_2Ni^{II}TPP + h\nu \rightarrow (CHA)Ni^{II}TPP + 2\ CHA \quad (5)$$

The photochemically produced $(CHA)_2Ni^{II}TPP$ and $Ni^{II}TPP$ disappear to achieve the equilibrium according to pseudo-first-order kinetics. It is noted that the transient is hardly detected at 1.7 M CHA, indicating that the photochemical formation of $(CHA)_2Ni^{II}TPP$ by eq 4 is canceled by the photochemical disappearance of $Ni^{II}TPP$ (eq 5).

The laser photolysis of $Ni^{II}TPP$ in toluene containing 0.5−8.2 M methylpyridines ($3\text{-}CH_3Py$ and $4\text{-}CH_3Py$) gives the results

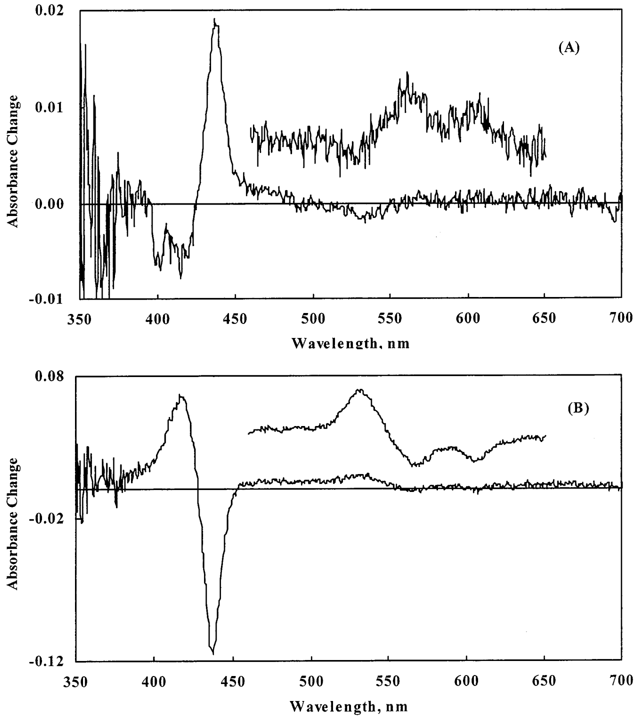

Figure 2. Transient absorption spectra observed at 300 K for Ni^{II}TPP in toluene containing (A) 0.88 and (B) 4.4 M cyclohexylamine, at 30 ns after the 355-nm laser pulse. The correct measurements of the absorbance change in the wavelengths $X < 430$ nm of the spectrum (A) could not be made because of the large absorbance of Ni^{II}TPP.

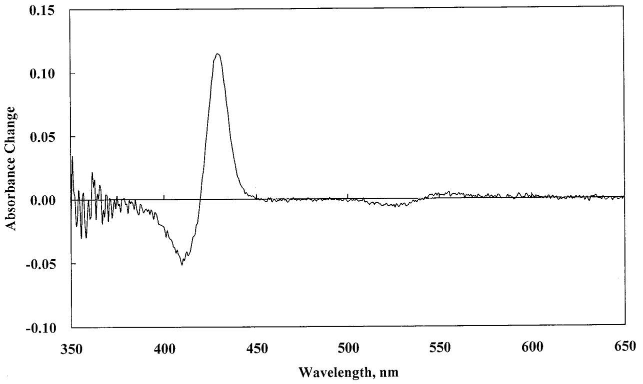

Figure 3. Transient absorption spectrum observed at 300 K for Ni^{II}TPP in toluene containing 7.7 M diethylamine at 30 ns after the 355-nm laser pulse.

similar to those obtained with CHA: the transient species changes from the six- to the four-coordinate species with an increase in the methylpyridine concentration.

As mentioned above, the secondary amines afford no effects on the absorption spectrum of Ni^{II}TPP even at high concentrations of the amines. Figure 3 shows the transient spectrum observed with the laser photolysis of Ni^{II}TPP in a diethylamine (DEA)−toluene solution. Because the spectrum has positive peaks at 430, 560, and 600 nm and negative ones at 413 and 525 nm, the transient is ascribed to the six coordinate species, (DEA)$_2$Ni^{II}TPP. These results are interpreted by assuming that Ni^{II}TPP associates two DEA molecules at the vacant axial positions in the excited state to yield (DEA)$_2$Ni^{II}TPP

$$\mathrm{Ni^{II}TPP} + h\nu + 2\mathrm{DEA} \rightarrow (\mathrm{DEA})_2\mathrm{Ni^{II}TPP} \qquad (6)$$

$$(\mathrm{DEA})_2\mathrm{Ni^{II}TPP} \rightarrow \mathrm{Ni^{II}TPP} + 2\ \mathrm{DEA} \qquad (7)$$

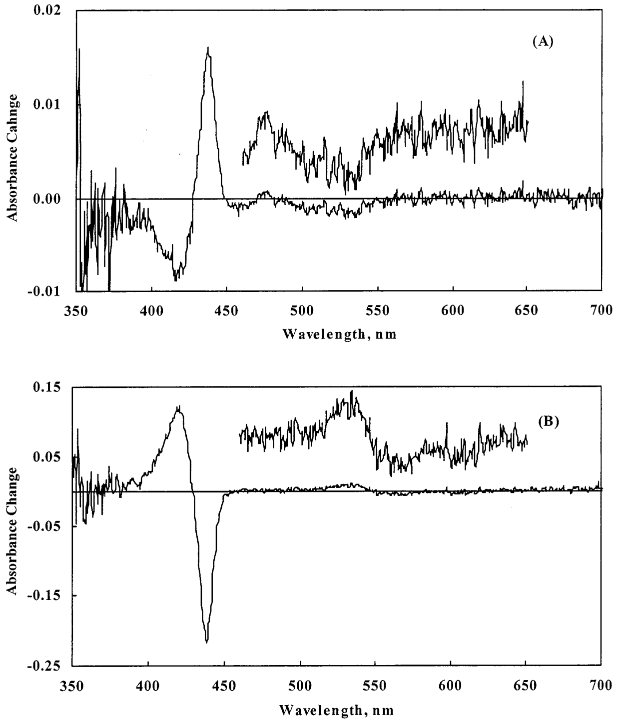

Figure 4. Transient absorption spectra observed at (A) 295 and (B) 220 K for Ni^{II}TPP in toluene containing 6.16 M 3-methylpyridine.

The photochemical formation of the six coordinate Ni^{II}TPP is also observed for the toluene solutions containing other secondary aliphatic amines, di-*n*-propylamine and di-*n*-butylamine.

The absorption spectrum of Ni^{II}TPP in toluene is not altered by the addition of tertiary amines similarly to the case of the secondary amines. Contrary to secondary amine−toluene solutions, no transient was observed for Ni^{II}TPP in tertiary amine−toluene solutions after the laser pulse in the amine concentration range 1.0−8.0 M. Probably, tertiary amines are unable to coordinate to the axial positions in both the ground and the excited state.

Transient Absorption Spectra at Low Temperatures. The color of the toluene solutions containing 1.0 M primary amines changes from orange red to violet with decreasing temperature. This result indicates that the six coordinate Ni^{II}TPP is produced at low temperatures owing to the shift of the equilibrium reactions (eqs 1 and 2) to the right side. The shift of the equilibrium at low temperatures is also observed for he toluene solution of Ni^{II}TPP in the presence of pyridine derivatives (3- and 4-methylpyridine).

Figure 4 shows the transient spectra observed for the toluene solution containing 6.16 M 3-methylpyridine, 3-MP, at 30 ns after the 355-nm laser pulse. The transient spectrum measured at 295 K has a positive peak at 430 nm and a negative one at 410 nm because of the photochemical formation of the six coordinate species, (3-MP)$_2$Ni^{II}TPP. At 220 K, the laser photolysis gives the transient spectrum identical with the difference spectrum, Ni^{II}TPP minus (3-MP)$_2$Ni^{II}TPP, indicating that (3-MP)$_2$Ni^{II}TPP photodissociates the axial ligands, 3-MP. These results imply that, on going from 295 to 220 K, the major light absorbing species in the solution changes from Ni^{II}TPP to (3-MP)$_2$Ni^{II}TPP.

Transient absorption spectra of Ni^{II}TPP in secondary amine (sec-amine)−toluene solutions were measured at low temperatures. The spectra taken at 200 K were found to be identical with those at 295 K. The absorption spectrum of Ni^{II}TPP in sec-amine−toluene at 200 K is identical with that of Ni^{II}TPP,

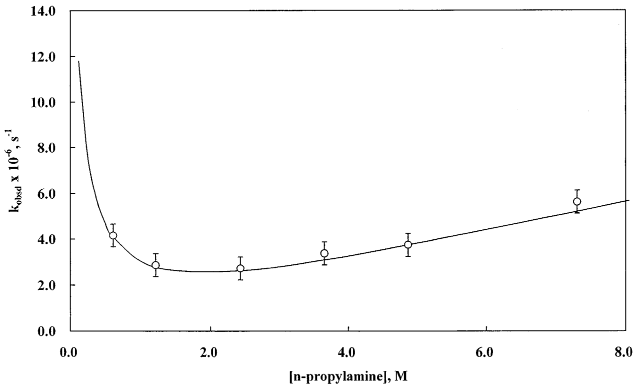

Figure 5. Rate constant for the decay of the transient measured at 295 K for $Ni^{II}TPP$ in toluene, represented as a function of [*n*-propylamine].

measured at 295 K. Thus, the species absorbing the laser pulse is solely ascribed to $Ni^{II}TPP$ independent of temperature in the range 200−295 K. Accordingly, the photoreaction in this system is interpreted in terms of the photochemical formation of the six-coordinate species, (sec-amine)$_2Ni^{II}TPP$, from $Ni^{II}TPP$.

No transient spectra were observed for tertiary amine− and 2-methylpyridine−toluene solutions of $Ni^{II}TPP$ in the temperature range 200−300 K. The tertiary amines studied here are triethylamine and tri-n- propylamine

Kinetic Studies of the Transient Species at 295 K. Figure 5 shows the pseudo-first-order rate constants, k_{obsd}, for the decay of the transient spectrum observed at 430 nm with the 355-nm laser photolysis of *n*-propylamine (*n*-PA)−toluene solutions of $Ni^{II}TPP$, represented as a function of the concentration of *n*-PA. The rate constants, k_{obsd}, obtained at 430 nm is almost identical with those at 410 nm. At 295 K, the rate constant, k_{obsd}, initially decreases toward a minimum value and then increases with an increase in [*n*-PA]. The general features of the plot of k_{obsd} vs the concentration of other primary amines and pyridine derivatives (3- and 4-methylpyridine) used in the present study are similar to the case of n-PA.

The laser photolysis of $Ni^{II}TPP$ in amine−toluene solutions affords nonequilibrium between four and six coordinate species of $Ni^{II}TPP$. Thus, the chemical reactions occurring after the photolysis are the processes to recover the equilibrium

$$\mathrm{Ni^{II}TPP} + \mathrm{amine} \underset{k_2}{\overset{k_1}{\rightleftarrows}} \mathrm{(amine)Ni^{II}TPP} \qquad (8)$$

$$\mathrm{(amine)Ni^{II}TPP} + \mathrm{amine} \underset{k_4}{\overset{k_3}{\rightleftarrows}} \mathrm{(amine)_2Ni^{II}TPP} \qquad (9)$$

By assuming the steady-state approximation with regard to the five coordinate species, (amine)$Ni^{II}TPP$, the pseudo-first-order rate constant, k_{obsd}, for, achievement of the equilibrium is formulated as

$$k_{obsd} = \frac{k_1k_3[\mathrm{amine}]^2 + k_2k_4}{k_2 + k_3[\mathrm{amine}]} \qquad (10)$$

The equilibrium constant K ($=k_1k_3/k_2k_4$) has already been obtained from the absorption spectral change of $Ni^{II}TPP$ in toluene solution containing amines. With the use of eq 10, K, and the least-squares fitting program, k_1, k_4, and $k_3/(k_2k_4)$ are determined from the plot of k_{obsd} vs [*n*-PA] in Figure 5: $K = 0.25$ M^{-2}, $k_1 = 6.7 \times 10^5$ $M^{-1}s^{-1}$, $k_4 = 2.54 \times 10^7$ s^{-1}, and $k_3/k_2 = 9.5$ M^{-1}. Unfortunately, the absolute values of k_2 and k_3 could not be determined in the present study. The solid curve in Figure 5 is the calculated one by eq 10 with the use of the kinetic parameters descried above.

TABLE 1: Rate and Equilibrium Constants for Association and Dissociation of Axial Amines

	k_1, $M^{-1}s^{-1}$	k_3/k_2, M^{-1}	k_4, s^{-1}	K,[a] M^{-2}
n-propylamine(r.t)	6.7×10^5	9.5	2.5×10^7	2.5×10^{-1}
n-buthylamine (r.t)	8.7×10^5	10.2	1.9×10^7	4.2×10^{-1}
isopropylamine (r.t)	5.3×10^5	10.5	2.0×10^8	2.8×10^{-2}
isobuthylamine (r.t)	6.3×10^5	18.6	6.5×10^7	1.8×10^{-1}
cycrohexylamine (r.t)	5.8×10^5	5.4	6.0×10^7	5.2×10^{-2}
diethylamine (r.t)			4.5×10^7	
dipropylamine (r.t)			2.7×10^7	
dibuthylamine (280K)			3.0×10^7	
3-methylpyridine (r.t)	1.4×10^6	2.6	9.8×10^7	3.7×10^{-2}
4-methylpyridine (r.t)	9.6×10^5	20.1	2.7×10^8	7.2×10^{-2}

[a] Experimental errors are wthin ±3%.

The pseudo-first-order rate constants, k_{obsd}, obtained with the laser photolysis of $Ni^{II}TPP$ in secondary amine−toluene solutions were measured in the concentration range 1.0−8.0 M at 295 K. It is found that k_{obsd} is invariable against the concentration of the amines. This finding suggests that the decay process of the six coordinate species produced by photolysis of $Ni^{II}TPP$ in secondary amine−toluene is principally the dissociation of the axial ligand: k_1[amine] and k_3[amine] are much smaller than k_2 and k_4. Accordingly, eq 10 is approximately changed to the following equation:

$$k_{obsd} = k_4 \qquad (11)$$

In Table 1 are listed the kinetic parameters, K, k_1, k_4, and k_3/k_2, obtained with the primary amines, secondary amines, and 3- and 4-methylpyridine at 295 K.

Rate Constant Measurements in the Temperature Range 220−300 K. As shown in eq 10, k_{obsd} is expressed by the rate constants, k_1−k_4. Because the rate constants are the functions of temperature, the plot of k_{obsd} vs the amine concentration is expected to display the characteristic curve dominated by the sample temperature. The plots of k_{obsd} vs the amine concentration were obtained with every 10 K step in the range 300−200 K for the primary, secondary, and aromatic amines.

Figure 6 shows the plots of k_{obsd} vs the concentration of isopropylamine, iso-PA, obtained with the laser photolysis of $Ni^{II}TPP$ in iso-PA−toluene solutions at 295 and 240 K. The k_{obsd} values obtained at 295 K decrease with a decrease in [iso-PA], and those at 220 K increase with an increase in [iso-PA].

To elucidate the plots of k_{obsd} vs [amine] in the temperature range 200−300 K, the rate constants, k_1−k_4, are formulated by the Arrhenius expression: $k_n = A_n \exp(-\Delta E_n/RT)$ $(n = 1-4)$. Thus, eq 10 is transformed to

$$k_{obsd} = \frac{A_{32}\ \exp(-\Delta E_{32}/RT)A_1\ \exp(-\Delta E_1/RT)\ [\mathrm{amine}]^2 + A_4\ \exp\{(-\Delta E_4)/RT\}}{1 + A_{32}\ \exp(-\Delta E_{32}/RT)[\mathrm{Amine}]} \qquad (12)$$

Here $A_{32} = A_3/A_2$ and $\Delta E_{32} = \Delta E_3 - \Delta E_2$. As mentioned above, the values of k_1, k_4, and k_2/k_3 were uniquely determined at $T = 295$ K. Thus, A_1, A_4, and A_{32} are respectively expressed as a function of ΔE_1, ΔE_4, and ΔE_{32}, leading to the conclusion that eq 12 has only three unknown parameters (ΔE_1, ΔE_4, and ΔE_{32}). Activation energies, ΔE_1, ΔE_4, and ΔE_{32}, were determined from the data of k_{obsd} and eq 12 with the use of the nonlinear least-squares fitting program. Then, pre-exponential factors are calculated from these activation energies. In the case of secondary amines, the rate constants, k_{obsd}, are independent of

TABLE 2: Kinetic and Thermodynamic Parameters for Association and Dissociation of Axial Amines

	ΔE_1, kcal	A_1, M^{-1}s^{-1}	ΔE_{32}, kcal	A_{32}, M^{-1}	ΔE_4, kcal	A_4, s^{-1}	ΔH, kcal	ΔS, eu
n-propylamine	3.1	1.3×10^8	−14.0	8.0×10^{-10}	3.8	1.6×10^{10}	−14.7	−51.5
n-buthylamine	3.2	2.0×10^8	−14.0	4.6×10^{-10}	3.0	8.7×10^{10}	−13.8	−55.2
isopropylamine	2.5	3.4×10^7	−0.9	2.3	13.0	3.2×10^{17}	−11.4	−44.3
isobuthylamine	3.7	3.2×10^8	−7.9	2.7×10^{-5}	12.0	2.1×10^{16}	-16.2	−57.0
cycrohexylamine	3.9	4.1×10^8	−0.4	2.7	9.8	9.3×10^{14}	−6.3	−27.3
diethylamine					4.5	1.5×10^{11}		
dipropylamine					5.0	5.6×10^{11}		
dibuthylamine					5.7	1.3×10^{12}		
3-methylpyridine	6.1	4.5×10^{10}	−5.7	1.7×10^{-4}	4.0	8.6×10^{10}	−3.6	−18.7
4-methylpyridin	5.0	4.6×10^9	−4.4	1.2×10^{-2}	4.0	2.3×10^{11}	−3.4	−16.7

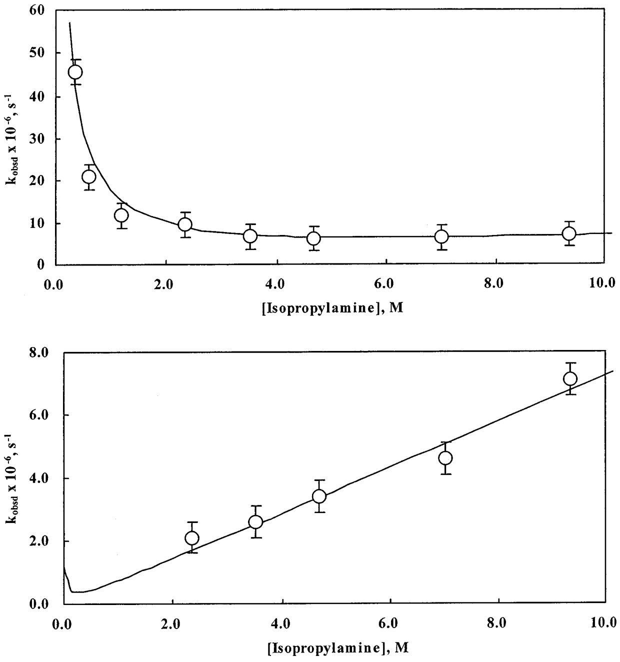

Figure 6. Rate constants for the decay of the transient measured at 295 and 220 K for Ni^{II}TPP in toluene, represented as a function of [isopropylamine].

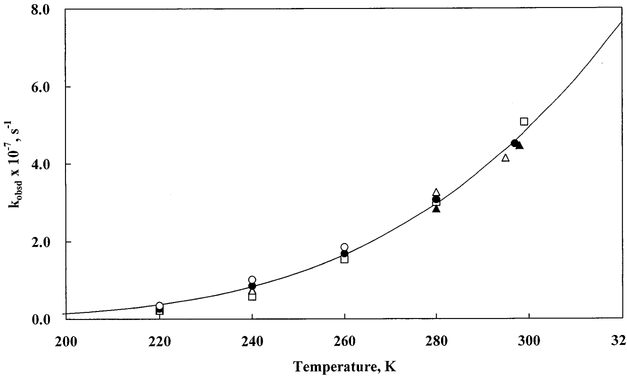

Figure 7. Rate constants for the decay of (DEA)$_2$Ni^{II}TPP for Ni^{II}TPP in toluene containing (open circle) 1.93, (closed circle) 2.90, (open triangle) 3.87, (closed triangle) 5.80, and (open square) 7.74 M diethylamine, represented as a function of temperature.

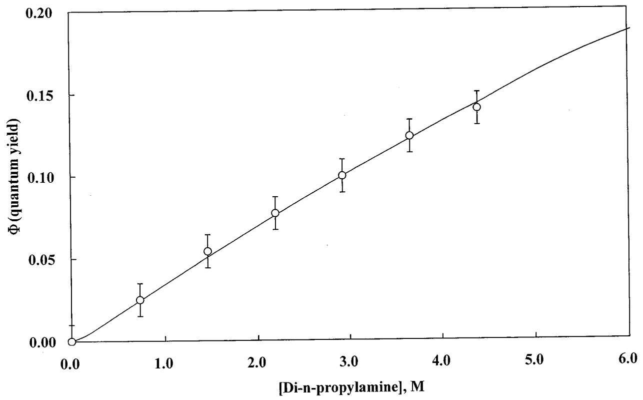

Figure 8. Quantum yields for the formation of (sec-DPA)$_2$Ni^{II}TPP from Ni^{II}TPP in toluene, represented as a function of [sec-DPA].

the concentration of the amines. From eq 12, the Arrhenius expression for k_{obsd} is simply written as

$$k_{obsd} = A_4 \exp(-\Delta E_4/RT) \tag{13}$$

Figure 7 exhibits the plots of k_{obsd} represented as a function of temperature at 1.93, 2.90, 3.87, 5.80, and 7.74 M diethylamine in toluene solutions. From the plots and the least-squares fitting program, A_4 and ΔE_4 are determined as $A_4 = 1.5 \times 10^{11}$ s^{-1} and $\Delta E_4 = 4.5 \times 10^3$ cal/mol. In Table 2 are listed A_1, A_{32}, A_4, ΔE_1, ΔE_{32}, ΔE_4, and ΔH for primary, secondary, and aromatic amines.

In a previous paper,[33] we have reported the laser photolysis studies of Ni^{II}TPP in a pyridine−toluene mixture in the temperature range 300−200 K. The transient observed by photolysis of (Py)$_2$Ni^{II}TPP at 220 K decayed according to pseudo-first-order kinetics with the rate constant k. On the basis of the fact that the plot of k vs [Py] gives a straight line with an intercept, the transient was assigned to the five coordinate species, (Py)Ni^{II}TPP. However, the present result indicates that the apparent linear plot of k vs [Py] can be obtained with the case that k_3[amine] $\gg$ k_2 (see eq 10). From Table 2, it is concluded that this case can be attained when the temperature of the sample solutions containing 1 M primary and aromatic amine becomes below 240 K. Thus, the earlier result can be reinterpreted: photolysis of (Py)$_2$Ni^{II}TPP gives Ni^{II}TPP, which returns to (Py)$_2$Ni^{II}TPP via the five coordinate (Py)Ni^{II}TPP.

Quantum Yield Measurements in Secondary Amine−Toluene Solutions. The quantum yield measurements for the formation of the six coordinate Ni^{II}TPP in di-*n*-propylamine (sec-DPA)−toluene solutions were carried out with the use of the laser photolysis technique. The method for determination of the quantum yields has already been described elsewhere.[22,47,48] The light quanta absorbed by Ni^{II}TPP were measured by monitoring the T−T absorption of Zn^{II}TPP in the standard benzene solution, which has the absorbance identical with that of Ni^{II}TPP in toluene.

Figure 8 shows the plot of the quantum yields for the formation of the six coordinate species, (sec-DPA)$_2$Ni^{II}TPP, at 300 K represented as a function of [sec-DPA]. The yield monotonically increases with an increase in [sec-DPA]. As will be discussed later, we consider that the photoinduced association and dissociation of axial amines take place according to the sequential mechanism. Thus, the photochemical reaction of

$Ni^{II}TPP$ in sec-DPA is represented by

$$\mathrm{Ni^{II}TPP(^1A_{1g})} + h\nu \rightarrow \mathrm{Ni^{II}TPP(^3B_{1g})} \qquad (14)$$

$$\mathrm{Ni^{II}TPP(^3B_{1g})} \xrightarrow{k_d} \mathrm{Ni^{II}TPP(^1A_{1g})} \qquad (15)$$

$$\mathrm{Ni^{II}TPP(^3B_{1g})} + \text{sec-DPA} \xrightarrow{k_a} \text{(sec-DPA)}\mathrm{Ni^{II}TPP(^3B_1)} \qquad (16)$$

$$\text{(sec-DPA)}\mathrm{Ni^{II}TPP\ (^3B_{1g})} \xrightarrow{k_b} \mathrm{Ni^{II}TPP\ (^1A_{1g})} + \text{sec-DPA} \qquad (17)$$

$$\text{(sec-DPA)}\mathrm{Ni^{II}TPP(^3B_1)} + \text{sec-DPA} \xrightarrow{k_c} \text{(sec-DPA)}\mathrm{Ni^{II}TPP(^3B_{1g})} \qquad (18)$$

The five coordinate nickel(II) porphyrins are known to have the $^3B_{1g}$ ground state.[40] From eqs 14−18, the yield, Φ, for the formation of $(\text{sec-DPA})_2Ni^{II}TPP$ is formulated as

$$\Phi = \Phi\ (^3B_{1g}) \frac{k_a[\text{sec-DPA}]}{k_d + k_a[\text{sec-DPA}]} \frac{k_c[\text{sec-DPA}]}{k_b + k_c[\text{sec-DPA}]} \qquad (19)$$

The quantum yield $\Phi(^3B_{1g})$ for the formation of the lowest excited state of $Ni^{II}TPP$ is assumed to be unity. With the use of the least-squares fitting program, we obtain $k_d/k_a = 25.0 \pm 1.0$ M and $k_b/k_c < 0.1$ M. Because the value, $1/k_d$, has been determined as ca. 250 ps by the femtosecond photolysis,[38] k_a is obtained as ca. 1.6×10^8 M^{-1} s^{-1}.[49] The exact value of k_b/k_c could not be determined because of the narrow concentration range of [sec-DPA].

Discussion

Nickel(II) porphyrins, $Ni^{II}P$, in noncoordinate solvents exhibit marked changes in the absorption spectra by the addition of nitrogeneous bases, N.[41−43] The absorption spectroscopic studies have demonstrated that the coordination of two nitrogeneous bases at the axial positions of $Ni^{II}P$ results in the change in the absorption spectra. The four- and six-coordinate species, $Ni^{II}P$ and $Ni^{II}P(N)_2$, have the spin state $S = 0$ and 1 at the ground states, respectively.[50] The NMR measurements of the porphyrin proton suggest that the intermediate five coordinate species, $Ni^{II}P(N)$ (either $S = 0$ or 1), plays a key role in establishment of the equilibrium reaction between $Ni^{II}P$ and $Ni^{II}P(N)_2$.[36,45]

The absorption spectral changes observed for primary amine−toluene solutions of $Ni^{II}TPP$ are in good agreement with those previously measured for solutions of nickel(II) porphyrins containing piperidine or pyridine.[33,41−43] The equilibrium constant, *K*, for the formation of bis−amine complexes of $Ni^{II}TPP$ increases in the order *n*-butylamine > *n*-propylamine > isobutylamine > cyclohexylamine > isopropylamine. This finding suggests that the branched-primary amines give the equilibrium constants smaller than linear-chain amines. It is noteworthy that the *K* values obtained with 3- and 4-methylpyridine are close to those of the branched primary amines.

The absorption spectrum of $Ni^{II}TPP$ in the toluene solution is not altered by the addition of secondary and tertiary amines in the temperature range 300−200 K. Presumably, the forward rate constant, k_3, for the formation of the six-coordinate species is very small because of crowded structures of the secondary and tertiary amines that prohibited the thermal coordination of the amines to the axial position of $Ni^{II}TPP$.

We have measured activation energies and frequency factors for k_4 processes. Among the amines studied, secondary amine systems afford large ΔE_4 and A_4 values for the dissociation of an axial amine molecule from the six-coordinate species, $(\text{sec-A})_2Ni^{II}TPP$. According to the transition state theory, k_4, is expressed by

$$k_4 = (kT/h)\chi \exp(\Delta S_4^*/R) \exp(-\Delta E_4/RT) \qquad (20)$$

where ΔS_4^* is the activation entropy and other symbols have their usual meanings. Thus, the large A_4 values ($A_4 \gg 10^{13}$ s^{-1}) obtained with the secondary amine systems are explained by a positive ΔS^* value at the transition state responsible for the dissociation of the axial amine. It is suggested that the transition state has a loose structure in comparison with that of the reactant, $(\text{sec-A})_2Ni^{II}TPP$. A large activation energies would be necessary for $(\text{sec-A})_2Ni^{II}TPP$ to attain such a loose transition state.

In primary amine−toluene solutions, $Ni^{II}TPP$ and the six-coordinate species, $(\text{pri-A})_2$ $Ni^{II}TPP$, exist as the equilibrium mixture. The laser photolysis of the solutions brings forth the nonequilibrium state because of the photochemical conversion of $(\text{pri-A})_2$ $Ni^{II}TPP$ to $Ni^{II}TPP$ or $Ni^{II}TPP$ to $(\text{pri-A})_2$ $Ni^{II}TPP$. The decay of the transients, therefore, is ascribed to the recovery of the equilibrium. The plots of the decay rate constants vs [pri-A] are well explained by assuming the steady-state approximation with regard to the five-coordinate species, $(\text{pri-A})Ni^{II}TPP$. These results lead to the conclusion that $(\text{pri-A})Ni^{II}TPP$ is highly unstable. It is likely that $(\text{pri-A})Ni^{II}TPP$ is readily transformed to either $Ni^{II}TPP$ by dissociation of the axial pri-A and/or $(\text{pri-A})_2Ni^{II}TPP$ by association of pri-A at the axial position. Similar observation has been made with the laser photolysis of the six coordinate iron(II) porphyrins. Bis−nitrogeneous base complexes of iron(II) porphyrins, $(N)_2Fe^{II}P$, photodissociate an axial N base to give the five coordinate species, $(N)Fe^{II}TPP$, which immediately undergoes “spontaneous dissociation” of another axial N base, resulting in the formation of the four coordinate $Fe^{II}P$.[4,13,51] The transient $Fe^{II}P$ returns to $(N)_2Fe^{II}TPP$ via $(N)Fe^{II}TPP$.

Photoexcited states of $Ni^{II}TPP$ and the six-coordinate complexes, $(N)_2Ni^{II}TPP$ (N = nitrogeneous bases), have been well studied by fast transient absorption and Raman spectroscopy.[7,37−40,50] The femtosecond photolysis[38] confirmed that (1) the lowest excited states, $^3B_{1g}$ ($^3(^1d_{x^2-y^2}, {}^1d_{z^2})$), of $Ni^{II}TPP$ having the lifetime of ca. 250 ps are produced within 350 fs after the pulse and (2) photoexcitation of $(N)_2Ni^{II}TPP$ initially gives the ligand excited state which decays to the $^1A_{1g}$ state ($^1(^2d_{z^2})$) within 20 ps. The lifetime of the $^1A_{1g}$ state of $(N)_2Ni^{II}TPP$ is too short to be detected owing to the ultrafast dissociation of the axial ligands.

It has been recognized that the $^3B_{1g}$ state of $Ni^{II}TPP$ can take two nitrogeneous ligands at the axial positions to give the ground state of $(N)_2Ni^{II}TPP$, and the $^1A_{1g}$ state of $(N)_2Ni^{II}TPP$ dissociates two axial nitrogeneous bases to yield $Ni^{II}TPP$ ($^1A_{1g}$).[38] The reaction mechanism for the formation of $(N)_2Ni^{II}TPP$ from $Ni^{II}TPP$ at the lowest excited state is considered to be either the synchronous or the sequential addition reaction of two N-base molecules at the axial positions. The synchronous addition mechanism seems very unlikely because it requires three body collision among $Ni^{II}TPP$ and two amine molecules. Thus, the sequential addition mechanism is more likely for interpretation of the formation of $(N)_2Ni^{II}TPP$ from the excited state of $Ni^{II}TPP$.

From the earlier and present studies,[3,34,35,40] the energetic diagram of the ground and the lowest excited states of $Ni^{II}TPP$, $(N)Ni^{II}TPP$, and $(N)_2Ni^{II}TPP$ are qualitatively described as shown in Scheme 1. The ground-state energy of $Ni^{II}TPP$ is 6−15 kcal higher than $(\text{pri-A})_2Ni^{II}TPP$ depending on the nature

SCHEME 1

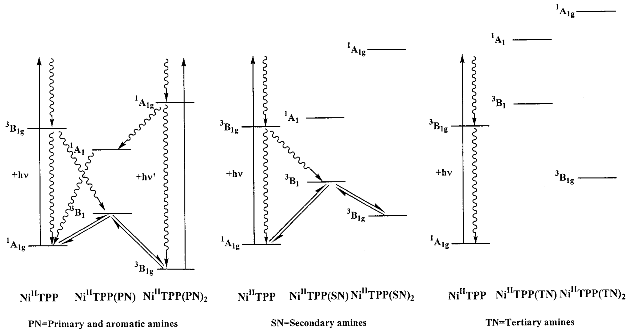

of the axial primary amine. In the case of the secondary and tertiary amines, the six-coordinate species, (sec-A)$_2$Ni^{II}TPP and (tert-A)$_2$Ni^{II}TPP, cannot be detected even at 200 K, indicating that the ground-state energy of Ni^{II}TPP is much lower than those of (sec-A)$_2$Ni^{II}TPP and (tert-A)$_2$Ni^{II}TPP. Presumably, owing to the bulky aliphatic groups, the secondary and tertiary amines suffer the strong strain energy by coordination to Ni^{II}TPP, and thus, the five- or six-coordinate species are hardly produced by thermal reactions.

With regard to pyridine derivatives, 3-methyl- and 4-methylpyridine can thermally coordinate to Ni^{II}TPP, resulting in the formation of the six-coordinate species. On the other hand, 2-methylpyridine hardly reacts with Ni^{II}TPP, suggesting that the methyl group at the 2 position of pyridine prohibits the interaction between the sp3 orbital of the N atom in 2-methylpyridine and the d_{z^2} orbital of the central Ni atom.

According to Scheme 1, the photodissociation of the two axial primary amine molecules sequentially occurs at the excited state: $^{1}A_{1g}$ of (pri-A)$_2$Ni^{II}TPP → $^{1}A_{1}$ of (pri-A)Ni^{II}TPP → $^{1}A_{1g}$ of Ni^{II}TPP. The sequential addition of two primary amines at the excited state of Ni^{II}TPP is represented as: $^{3}B_{1g}$ of Ni^{II}TPP → $^{3}B_{1}$ of (pri-A)Ni^{II}TPP → either $^{3}B_{1g}$ of (pri-A)$_2$Ni^{II}TPP or $^{1}A_{1g}$ of Ni^{II}TPP.

In secondary amine−toluene solutions of Ni^{II}TPP, the relaxation pathways of the excitation energy leading to the association of the amine molecules at the axial positions are $^{3}B_{1g}$ of Ni^{II}TPP → $^{3}B_{1g}$ of (sec-A)Ni^{II}TPP → either $^{3}B_{1g}$ of (sec-A)$_2$Ni^{II}TPP or $^{1}A_{1g}$ of Ni^{II}TPP.

It is found that neither the thermal nor photochemical reactions of Ni^{II}TPP in tertiary amine−toluene solutions gives (tert-A)$_2$Ni^{II}TPP. This finding implies that, as shown in Scheme 1, the $^{3}B_{1}$ state of (tert-A)Ni^{II}TPP is higher in energy than the $^{3}B_{1g}$ state of Ni^{II}TPP, and the $^{3}B_{1g}$ state of (tert-A)$_2$Ni^{II}TPP is higher in energy than the $^{1}A_{1g}$ state of Ni^{II}TPP.

References and Notes

(1) Hoshino, M. *Chem. Phys. Lett.* **1985**, *120*, 50−52.

(2) Hoshino, M.; Arai, S.; Yamaji, M.; Hama, Y. *J. Phys. Chem.* **1986**, *90*, 2109−2111.

(3) Kim, D.; Kirmaier, C.; Holten, D. *Chem. Phys.* **1983**, *75*, 305−322.

(4) White, D. K.; Cannon, J. B.; Traylor, T. J. *J. Am. Chem. Soc.* **1979**, *101*, 2443−2454.

(5) Hoshino, M.; Ida, H.; Yasufuku, K.; Tanaka, K. *J. Phys. Chem.* **1986**, *90*, 3984−3987.

(6) Hoshino, M.; Kogure, M. *J. Phys. Chem.* **1989**, *93*, 5478−5484.

(7) Tait, C. D.; Hoten, D.; Gouterman, M. *Chem. Phys. Lett.* **1983**, *100*, 268−272.

(8) Kendrick, M. J.; AI-Akdar, W. *Inorg. Chem.* **1987**, *26*, 3971−3972.

(9) Tetreau, C,; Lavalette, D.; Momenteau, M. *J. Am. Chem. Soc.* **1983**, *105*, 1506−1509.

(10) Hoshino, M.; Kogure, M.; Amano, K.; Hinohara, T. *J. Phys. Chem.* **1989**, *93*, 6655−6659.

(11) Vogler, A.; Kunkelt, H. *Bunsen-Ges. Phys. Chem.* **1976**, *80*, 425−429.

(12) Yamaji; M.; Hama, Y.; Hoshino, M. *Chem. Phys. Lett.* **1990**, *165*, 309−314.

(13) Hoshino, M.; Ueda, K.; Takahashi, M.; Yamaji, M.; Hama, Y.; Miyazaki, K. *J. Phys. Chem.* **1992**, *96*, 8863−8870.

(14) Hoshino, M.; Seki, H.; Yamaji, M.; Hama, Y. *Photochem. Photobiol.* **1993**, *57*, 728−731.

(15) Collman, J. P.; Gagne, R. R.; Reed, C. A.; Halbert, T. R.; Lang, G.; Robinson, W. J. *J. Am. Chem. Soc.* **1975**, *97*, 1427−1439.

(16) Ledon, H.; Bonnet, M. *J. Chem. Soc. Chem. Commun.* **1979**, 702−704.

(17) Hoshino, M.; Nagamori, T.; Seki, H.; Chihara, T.; Tase, T.; Wakatsuki, Y.; Inamo, M. *J. Phys. Chem. A* **1998**, *102*, 1297−1301.

(18) Hoshino, M.; Sonoki, H.; Miyazaki, Y.; Iimura, Y.; Yamamoto, K. *Inorg. Chem.* **2000**, *39*, 4850−4857.

(19) Adachi, H.; Sonoki, H.; Hoshino, M.; Wakasa, M.; Hayashi, H. *J. Phys. Chem. A* **2001**, *105*, 392−398.

(20) White, D. K.; Cannon, J. B.; Traylor, T. G. *J. Am. Chem. Soc.* **1979**, *101*, 2443−2454.

(21) Cornelius, P. A.; Hochstrasser, R. M.; Steele, A. W. *J. Mol. Biol.* **1983**, *163*, 119−128.

(22) Hoshino, M.; Ozawa, K.; Seki, H.; Ford, P. C. *J. Am. Chem. Soc.* **1993**, *115*, 9568−9575.

(23) Philo, J. S.; Larry, J. W. *J. Biol. Chem.* **1990**, *265*, 139−143.

(24) Mathews, A. J.; Rolfs, R. J.; Olson, J. T.; Tame, J.; Renaud, J.-P. J. *Biol. Chem.* **1989**, *264*, 16573−16583.

(25) Gibson, Q. H.; Edelstein, S. J. *J. Biol. Chem.* **1987**, *262*, 516−519.

(26) Chernoff, D. A.; Hochstrasser, R. M. Steele, A. W. *Proc. Natl. Acad. Sci. U.S.A.* **1980**, *77*, 5606−5610.

(27) Ferrone, F. A.; Martino, A. J.; Basak, S. *Biophys. J.* **1985**, *48*, 269−282.

(28) Martin, J. L.; Migus, A.; Poyat, C.; Lecarpentier, Y.; Astier, R.; Antonetti, A. *EMBO J.* **1983**, *12*, 1815−1819.

(29) Goldbeck, R. A.; Paquette, S. J.; Bjorling, S. C.; Klinger, D. S. *Biochemistry* **1996**, *35*, 8628−8639.

(30) Hoshino, M.; Sonoki, H.; Suzuki, H.; Adachi, H.; Miyazaki, Y.; Yamanaka, K. *J. Phys. Chem. B* **2001**, *44*, 10976−10982.

(31) Hoshino, M.; Hirai, T. *J. Phys. Chem.* **1987**, *91*, 4510−4514.

(32) Yamauchi, S.; Suzuki, Y.; Ueda, T.; Akiyama, K.; Ohba, Y.; Imaizumi, M. *Chem. Phys. Lett.* **1995**, *232*, 121−126.

(33) Hoshino, M. *Inorg. Chem.* **1986**, *25*, 2476−2478.

(34) Acke, R. K.; Gouterman, M. *Theor. Chim. Acta* **1970**, *17*, 408−416.

(35) Antipas, A.; Gouterman, M. *J. Am. Chem. Soc.* **1983**, *105*, 4896−4901.

(36) La Mar, G. N.; Walker, F. A. In *The Porphyrins*; Dolphine, D., Ed.; Academic: New York, 1979; Vol. IV, Chapter 2.

(37) Eom, H. S.; Jeoung, S. C.; Kim, D.; Ha, J.-H.; Kim, Y.-R. *J. Phys. Chem. A* **1977**, *101*, 3661−3669.

(38) Rodriguez, J.; Holten, D. *J. Chem. Phys.* **1990**, *92*, 5944−5949.

(39) Drain, C. M.; Gentemann, S.; Robert, J. A.; Nelson, N. Y.; Medforth, C. J.; Jia, S.; Simpson, M. C.; Smith, K. M.; Fajer, J.; Shelnutt, J. A.; Holten, D. *J. Am. Chem. Soc.* **1998**, *120*, 3781−3791.

(40) Findsen, E. W.; Alston, K.; Shelnutt, J. A.; Ondrias, M. R. *J. Am. Chem. Soc.* **1986**, *108*, 4009−4017.

(41) Walker, F. A.; Hui, E.; Walker, J. M. *J. Am. Chem. Soc.* **1975**, *97*, 2390−2397.

(42) Baker, E. W.; Brookhart, M. S.; Corwin, A. H. *J. Am. Chem. Soc.* **1964**, *86*, 4587−4591.

(43) Mclees, B. D.; Caughey, W. S. *Biochemistry* **1968**, *7*, 642−652.

(44) Choi, S.; Phillips, J. A.; Ware, W., Jr.; Wittschieben, C.; Medforth, C. J.; Smith, K. M. *Inorg. Chem.* **1994**, *33*, 3873−3876.

(45) Abraham, R. J.; Swinton, P. F. *J. Chem. Soc. B* **1969**, 903−908.

(46) Yue, K. T.; Lin, M.; Gray, T. A.; Marzilli, L. G. *Inorg. Chem.* **1991**, *30*, 3214−3222.

(47) Adachi, H.; Suzuki, H.; Miyazaki, Y.; Iimura, Y.; Hoshino, M. *Inorg. Chem.* **2002**, *41*, 2158−2524.

(48) Seki, H.; Okada, K.; Iimura, Y.; Hoshino, M. J. *Phys. Chem. A* **1977**, *101*, 8174−8178.

(49) We can also obtain $k_d/k_a < 0.1$ M and $k_b/k_c = 25$ M from the plot in Figure 8 and eq 19. The former value gives $k_a > 4.0 \times 1010$ M^{-1} s^{-1}, which clearly exceeds the limit of the diffusion controlled process. We, thus, discard the values of $k_d/k_a < 0.1$ M and $k_b/k_c = 25$ M.

(50) Findsen, E. W.; Shelnutt, J. A.; Friedman, J. M.; Ondrias, M. R. *Chem. Phys. Lett.* **1986**, *126*, 465−471.

(51) Lavalette, D.; Tetreau, C. Momenteau, M. *J. Am. Chem. Soc.* **1979**, *101*, 5395−5401.